Journal of Polymers and the Environment
https://doi.org/10.1007/s10924-023-02813-1

ORIGINAL PAPER

# Eugenol-DOPO: A Bio-Based Phosphorous-Containing Monomer for Thiol-ene Photocurable Thermosets

**Ozge Ozukanar[1] · Emrah Çakmakçi[2] · Gokhan Sagdic[1] · Ufuk Saim Gunay[1] · Hakan Durmaz[1] · Volkan Kumbaraci[1]**

Accepted: 20 February 2023


## Abstract

The adverse health and environmental effects of petroleum-based materials have become a driving force for the fabrication of bio-based monomers. In this study, we synthesized a novel bio-based reactive phosphorus-containing; eugenol-DOPO, which was prepared in one step by the reaction of 9,10-dihydro-9-oxa-10-phosphaphenanthrene-10-oxide (DOPO) and eugenol via Atherton–Todd reaction. Moreover, a diallyl compound was also prepared by using eugenol and piperazine. All monomers were characterized by nuclear magnetic resonance (NMR), mass, and Fourier-transform infrared (FTIR) spectroscopies. Thiol-ene photocured polysulfide thermoset networks were prepared by using these newly synthesized bio-based monomers. Thermal and thermomechanical properties of the thermosets were measured. Photo-crosslinked networks displayed over 88% gel content values. The thermal stability of the networks as well as the resulting char yields were improved as the percentage of eugenol-DOPO was increased in the formulations. The presence of N and P played a synergistic effect and the limiting oxygen index (LOI) values for the thermoset materials were enhanced. We believe eugenol-DOPO is not only a good alternative monomer for the preparation of thermally stable photocurable thermosets, but it is also a suitable bio-based additive for other polymers as well.

## Graphical Abstract

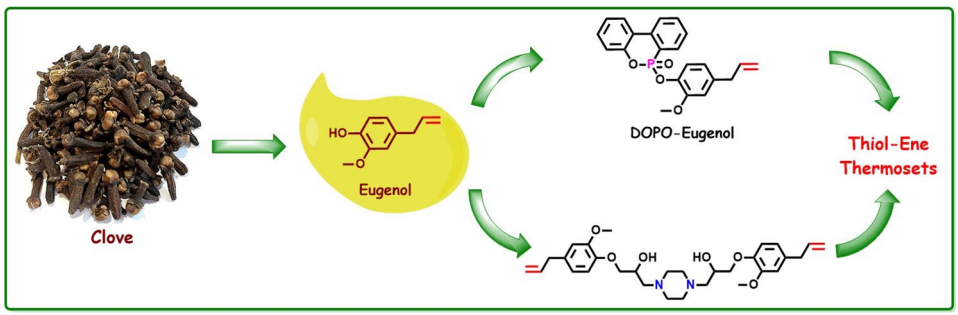


**Keywords** Eugenol · Piperazine · DOPO · Thiol-ene · Thermoset

## Introduction

In recent years, concerns about the environmental problems related to the use of petroleum-based materials have led to numerous studies on the development of bio-based alternative materials [1–8]. In accordance with this purpose, many biomass-derived building blocks such as vegetable oils [9, 10], isosorbide [11–13], furan [14, 15], vanillin [16, 17], itaconic acid [18], pyrogallol [19], eugenol [20–23], etc.,

✉ Emrah Çakmakçi
emrah.cakmakci@marmara.edu.tr

✉ Volkan Kumbaraci
kumbaracii@itu.edu.tr

[1] Department of Chemistry, Istanbul Technical University, 34469 Istanbul, Turkey

[2] Department of Chemistry, Marmara University, 34722 Istanbul, Turkey

Published online: 15 March 2023

have been utilized for the fabrication of several monomers, polymers or additives.

While most of these bio-based building blocks need to be functionalized with allyl, vinyl, acrylate, methacrylate or thiol groups to be used for thiol-ene photopolymerization (TEP), among them eugenol is particularly intriguing for TEP since it already has an allyl group, eliminating the functionalization step with relatively toxic allyl bromide/allylchloride, acryloyl chloride or such reactants [23]. TEP is a remarkable photocuring method that outperforms traditional photocuring systems owing to its unique characteristics such as photoinitiatorless curing, homogeneous network formation, reduced oxygen inhibition, high conversion rates, etc. [24–30].

Eugenol is an abundant, cheap building block that is mainly extracted from clove oil. It bears an aromatic ring, a phenolic –OH group and as noted above, an allyl group [31–33]. Previously, eugenol was successfully used for the preparation of photocured materials [33–37]. For instance, Modjinou et al., synthesized allyl-eugenol, a difunctional allyl derivative, and then prepared antibacterial and antioxidant bio-based networks therefrom by using TEP [36]. The thermosets displayed high double bond conversion values and low glass transition temperatures (*Tgs*). Similarly, Dai et al., prepared thiol-ene photocured networks by using the same monomer (allyl-eugenol) and diallyl itaconate [37]. As the percentage of diallyl itaconate was increased in the thermosets, the gel content, *Tg*s, and modulus values were improved. Moreover, these networks exhibited antibacterial properties.

The design and synthesis of flame retardant monomers for TEP is an active area of research, hence several flame retardant monomers containing P, B, Si, and/or N elements have been prepared in literature for TEP [14, 26, 27, 38]. With the rise of the "*Green Chemistry*" concept in polymer science, researchers have begun to focus on bio-based or bio-derived flame retardants [39–42]. Starch, vegetable oil, chitosan, cellulose, cardanol, lignin, alginate, proteins, phytic acid, and deoxyribonucleic acid (DNA), etc., can be used with or without modification as flame retardants [41, 42]. Previously, eugenol was also utilized for the preparation of bio-based flame retardants [43–51]. For instance; Miao et al., reacted eugenol with phosphorus oxychloride to synthesize a trifunctional allyl compound (TAMPP) [50]. This monomer when used in TEP resulted in highly thermally stable networks with char yields over 30% at 800 °C under nitrogen atmosphere, indicating good flame retardancy. When TAMPP was used with bismaleimide resins, LOI values as high as 39.6% were reached [51].

In this work, we synthesized a novel P-containing reactive monomer; eugenol-DOPO. This monomer was synthesized in one step by the reaction of eugenol with DOPO via the Atherton–Todd reaction. DOPO is a well-known and widely studied flame retardant additive/precursor. Furthermore, a diallyl compound was also synthesized from eugenol and piperazine. Here, these monomers were used in conjunction with commercial allyl and thiol compounds, and thiol-ene photocured thermosets were prepared.

## Experimental

### Materials

Anhydrous sodium sulfate, triethyl amine ($Et_3N$), sodium chloride, sodium hydroxide (NaOH), tetrabutylammonium bromide (TBAB), piperazine, eugenol (98%), epichlorohydrin (ECH), carbon tetrachloride ($CCl_4$), dichloromethane (DCM), ethyl acetate, hexane, chloroform ($CHCl_3$), glyoxal bis(diallyl acetal) (GBDA), and trimethylolpropane tris(3-mercapto propionate) (3SH) were purchased from Sigma Aldrich. 9,10-Dihydro-9-oxa-10-phosphaphenanthrene 10-oxide (DOPO) was purchased from TCI and 2-hydroxy-2-methyl-1-phenyl-1-propanone (Darocur 1173) was obtained from BASF. All solvents were of HPLC or ACS grade. Purifications via column chromatography were performed with silica gel 60 (Merck, 0.040–0.063 mm) which has 230–400 mesh ASTM and Celite®. Analytical thin layer chromatography (TLC) was performed on Merck labeled silica gel (60 HF254, 90% < 55 µm) plates (0.25 mm) pre-coated with a fluorescent indicator, and preparative plate chromatography purifications were performed on silica gel plates (750.0 µm) pre-coated with a fluorescent indicator. Visualization was affected with 254 nm ultraviolet light and iodine on silica.

### Characterization Methods

FTIR spectra were recorded on a Cary 630 FTIR (Agilent Technologies) instrument over the range of $4000-600\ cm^{-1}$. $^{1}H$ NMR (500 MHz) and $^{13}C$ NMR (125 MHz) spectra were recorded using an Agilent VNMRS 500 instrument in $CDCl_3$. $^{31}P$ NMR (162 MHz) spectra were recorded using a Varian 400 instrument in $CDCl_3$. The abbreviations used for the NMR multiplicities are as follows: s = singlet, bs = broad singlet, dd = doublet of doublets, d = doublet, ddt = doublet of doublet of triplets, ddd = doublet of doublet of doublet, t = triplet, tdd = triplet of doublets of doublets, and m = multiplet. Ultra Performance Liquid Chromatography (UPLC-QTof) measurements, which was equipped with mass spectrometry, were performed by using Waters (Acquity H Class Plus) UPLC instrument equipped with Vion IMS QTof. Dynamic mechanical analysis (DMA) was performed on a PerkinElmer DMA 8000 analyzer in tension mode. Samples ($40\times10\times0.1$ mm) were clamped, and strain was applied at a frequency of 1 Hz and a heating of 3 °C/min from − 5

**Scheme 1** Synthesis of EECH and BEECH

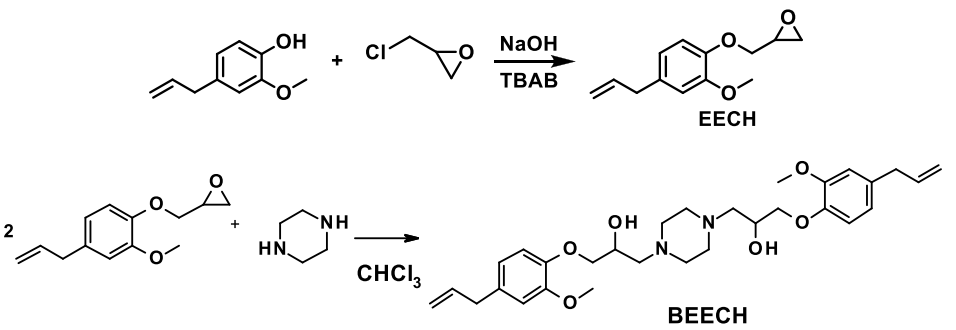


to 100 °C. Differential scanning calorimetry (DSC) experiments were performed under a nitrogen atmosphere on the PerkinElmer Pyris Diamond DSC apparatus. Samples were kept at − 30 °C for 2 min and then heated to 60 °C with a heating rate of 20 °C/min. After holding for 2 min at this temperature, samples were cooled to -30 °C with a cooling rate of 20 °C/min, followed by keeping at this temperature for 2 min. Finally, they were reheated to 60 °C with a heating rate of 20 °C/min. Data from the second heating cycle were reported. Thermogravimetric analyses (TGA) of the photocured films were performed by using a PerkinElmer thermogravimetric analyzer (Pyris 1 TGA model). Samples were run from 30 to 600 °C with a heating rate of 10 °C/min under a nitrogen atmosphere. The water contact angles (CA) of the coatings were determined on a Kruss (Easy Drop DSA-2) tensiometer. Measurements were made using 3 − 5 µL drops of distilled water. For each sample, at least three measurements were made, and the average was taken. The transmission spectra of the networks were obtained by using a Shimadzu 3100 UV–vis-NIR spectrometer. Gel contents of the coatings were determined by soxhlet extraction of the pre-weighted films for 24 h with chloroform. The insoluble gel fraction was dried in a vacuum oven at 40 °C to constant weight and the gel percentage was calculated. LOI values of the thermosets were measured by using an FTT (Fire Testing Technology) type instrument, according to ASTM D2863-08.

## Synthesis of Eugenyl Glycidylether (EECH)

The synthesis was performed according to the literature [52]. Eugenol (5 g, 30.45 mmol), ECH (11.27 g, 121.80 mmol), and TBAB (0.98 g 3.04 mmol) were stirred in a 100 mL round-bottom flask at 100 °C for 1 h. Then, the mixture was cooled down to room temperature and 12 mL of an aqueous solution of 20% NaOH (2.44 g/12.2 mL water) and TBAB (1 g, 3.04 mmol) were added to this mixture and the solution was stirred for 2 h. After that, 30 mL of ethyl acetate was added to the mixture, and the organic layer was washed with water, dried with sodium sulfate, and evaporated to dryness in vacuum. The crude product was purified by column chromatography over silica gel (hexane/ethyl acetate, 8/2), yielding the product as a pale yellow liquid (yield: 6.03 g, 90%).

$^{1}$H-NMR ($CDCl_3$, δ): 6.86 (d, J = 8.1 Hz, 1H, Ar), 6.71 (s, 1H, Ar) 6.70 (d, J = 8.1 Hz, 1H, Ar), 5.94 (m, 1H, CH), 5.05 (m 2H, $CH_2$), 4.20 (dd, J = 11.4, 3.5 Hz, 1H), 3.99 (dd, J = 11.4, 5.6 Hz, 1H), 3.84 (s, 3H, $OCH_3$), 3.33 (m, 1H, OCH), 3.32 (d, J = 6.7 Hz, 2H, $ArCH_2$), 2.86 (t, J = 4.5 Hz, 1H, $OCH_2$), 2.71(m, 1H, $OCH_2$).

$^{13}$C-NMR ($CDCl_3$, δ): 149.60, 146.35, 137.55, 133.88, 120.52, 115.71, 114.46, 112.47, 70.48, 55.87, 50.26, 44.91, 39.81.

FT-IR ($cm^{-1}$): 3030, 3000, 2926, 1638, 1584, 1507, 1476, 1138, 1258, 1226, 1028, 900.

## Synthesis of Bis EECH (BEECH)

Into 250 mL of round-bottom flask were added EECH (5 g, 22.7 mmol), piperazine (1.0 g, 11.89 mmol), and $CHCl_3$ (50 mL), respectively. The mixture was refluxed for 6 h, then cooled to room temperature and stirred overnight at room temperature. The mixture was taken to a separatory funnel and extracted with water two times to remove excess piperazine. Next, the organic phase was dried with sodium sulfate, filtered, and evaporated to dryness. The obtained product was further purified by column chromatography over silica gel (hexane/ethyl acetate, 6/4) to give the product as a yellow sticky solid (yield: 5.5 g, 92%). The syntheses of EECH and BEECH are depicted in Scheme 1.

$^{1}$H-NMR ($CDCl_3$, δ): δ 6.86 (d, J = 8.1 Hz, 2H, Ar), 6.71 (s, 2H, Ar) 6.70 (d, J = 8.1 Hz, 2H, Ar), 5.94 (m, 2H, CH), 5.05 (m 4H, $CH_2$), 4.12 (bs, 2H, $OCH_2$), 4.0 (bs, 4H, $OCH_2$, OCH), 3.83 (s, 6H, $OCH_3$), 3.33 (d, 2H, $ArCH_2$), 2.88–2.32 (m, 14H, $OCH_2$).

$^{13}$C-NMR ($CDCl_3$, δ): 149.71, 146.64, 137.58, 133.74, 120.57, 115.69, 114.78, 112.45, 72.61, 65.89, 65.68, 61.28, 60.57, 55.85, 54.66, 53.39, 46.06, 39.83.

FTIR ($cm^{-1}$): 3319, 2933, 1638, 1587, 1507, 1470, 1258, 1228, 1138, 1028, 900.

ESI–MS, m/z $C_{30}H_{42}N_2O_6$ calculated: 526.3043; Found: 527.3155 $[M+H]^+$.

## Synthesis of E-DOPO

Into a 250 mL of round-bottom flask were added DOPO (5 g, 23.13 mmol), $Et_3N$ (2.7 g, 26.48 mmol) and dissolved with DCM (20 mL) and stirred at room temperature for 30 min. Next, the solution was cooled to 0 °C, and eugenol (4.0 g, 24.36 mmol) was added to this solution and stirred for 30 min, followed by the drop-wise addition of $CCl_4$ (4.07 g, 26.48 mmol) via a dropping funnel at this temperature. The mixture was allowed to stir at 0 °C for 30 min and 24 h at room temperature. The mixture was taken to a separatory funnel and extracted with water (3 × 100 mL), combined organic phases were dried with sodium sulfate, filtered, and evaporated to dryness to give an oil. The obtained oil was dissolved in $CHCl_3$ and precipitated into cold hexane and the excess solvent was decanted, yielding a pale yellow oil (yield: 5.08 g, 58%) (Scheme 2).

$^1$H-NMR ($CDCl_3$, δ): δ 8.06 (ddd, J = 14.8, 7.6, 1.4 Hz, 1H, Ar), 8.01–7.94 (m, 1H, Ar), 7.94 (dd, J = 7.9, 1.6 Hz, 1H, Ar), 7.73 (ddt, J = 8.2, 7.5, 1.3 Hz, 1H, Ar), 7.51 (tdd, J = 7.6, 3.8, 1.0 Hz, 1H, Ar), 7.39 (ddt, J = 8.5, 7.3, 1.4 Hz, 1H), 7.31–7.24 (m, 1H), 7.24 (dd, J = 8.1, 1.3 Hz, 1H), 7.12 (dd, J = 8.2, 1.8 Hz, 1H), 6.66 (dd, J = 8.1, 2.0 Hz, 1H), 6.61 (d, J = 2.0 Hz, 1H), 5.97–5.85 (m, 1H), 5.09–5.00 (m, 2H), 3.55 (s, 3H), 3.33–3.26 (m, 2H).

$^{13}$C-NMR ($CDCl_3$, δ): 150.53, 150.23, 150.17, 138.19, 137.28, 137.10, 137.01, 133.61, 130.86, 130.35, 128.13, 125.09, 124.69, 123.90, 122.77, 122.13, 121.32, 120.62, 120.37, 116.07, 112.76, 55.51, 39.91.

FTIR ($cm^{-1}$): 3065.7, 3002.4, 2834.6, 1595.3, 1505.8, 1269.2, 1192.7, 1116.3, 1034.3, 995.2, 915.1, 792.1, 751.1, 602.0, 518.1, 501.3

$^{31}$P-NMR (471 MHz, $CDCl_3$) (ppm): 6.89.

ESI–MS, m/z $C_{22}H_{19}O_4P$ calculated for: 378.1021; Found: 379.1100, $[M+H]^+$.

## Preparation of Thiol-ene Photocured Thermosets

Several formulations were prepared by mixing the reactant monomers according to the ratios given in Table 1. The monomers were weighed into an aluminum foil wrapped beaker, and all monomers were mixed until homogenization. For BEECH-containing formulations, a small amount of (0.5–1 mL) DCM was added to aid it to dissolve in the mixture. Finally, a 3 wt.% (with respect to the total weight of the monomers) photoinitiator was added to the mixture. The uniform mixtures were poured into Teflon molds and were cured under UV irradiation (OSRAM, 300W, $\lambda_{max}$ = 365 nm, 10 mW/cm$^2$) for 3 min. The samples were encoded as GTEBX where, G, T, E, and B represent, GBDA, 3SH, E-DOPO, and BEECH, respectively. X represents the molar amount of E-DOPO (or BEECH) in the formulations.

**Scheme 2** Synthesis of E-DOPO

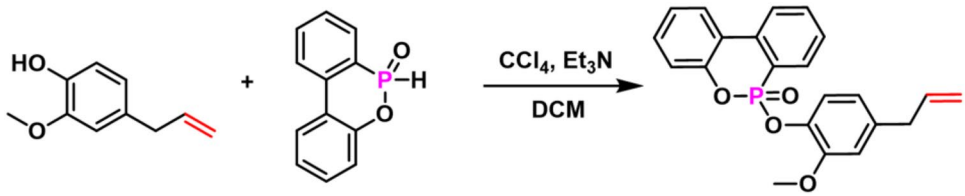


**Table 1** Recipe for the photocurable compositions[a]

| | GDBA (mmol) | 3SH (mmol) | E-DOPO (mmol) | BEECH (mmol) | E-DOPO (%) | P (%)[b] | Gel content (%) |
|---|---|---|---|---|---|---|---|
| GT | 3.00 | 4 | – | – | 0.0 | – | 97 |
| GTE0.25 | 2.94 | 4 | 0.25 | – | 63 | 0.32 | 94 |
| GTEB0.25 | 2.81 | 4 | 0.25 | 0.25 | 35 | 0.30 (0.28) | 92 |
| GTE0.5 | 2.88 | 4 | 0.5 | – | 46 | 0.62 | 91 |
| GTE1.0 | 2.75 | 4 | 1.0 | – | 54 | 1.18 | 92 |
| GTEB1.0 | 2.25 | 4 | 1.0 | 1.0 | 44 | 1.00 (0.91) | 88 |

[a]3% Darocur 1173 (with respect to the total weight of all monomers) was added to each formulation

[b]The numbers in parentheses display the N percentages

## Results and Discussion

### Characterization of the Synthesized Monomers

In this work, two novel eugenol-based and allyl-functional monomers were synthesized. BEECH was synthesized in two steps. First, eugenol was reacted with ECH to give EECH which was then reacted with piperazine to produce a di-allyl functional nitrogen-containing monomer (BEECH). Eugenol-DOPO (E-DOPO), which is a phosphorus-containing mono-allyl functional monomer, was prepared in a single step by the Atherton–Todd reaction. All synthesized monomers were characterized by NMR and FTIR measurements. The $^{1}$H-NMR and $^{13}$C-NMR of EECH are given in Figs. S1 and S2, respectively. While the aromatic hydrogens of EECH (Fig. S1) resonated between 7.0 and 6.5 ppm, the allylic hydrogens were observed at 6.0 and 5.0 ppm [43, 53]. The chemical shifts of the hydrogens attached to the oxirane ring were detected between 3.5 and 2.5 ppm [53]. $^{13}$C-NMR of EECH was also recorded and further confirmed the structure and purity of this precursor (Fig. S2). BEECH was obtained from the ring opening reaction of EECH with piperazine.

Similar to the $^{1}$H-NMR spectrum of EECH, BEECH displayed the aromatic protons in the downfield region (7.0–6.5 ppm), and the peaks at 5.94 and 5.05 ppm were assigned to the double bond protons (Fig. 1). Due to the ring opening of the epoxide groups, $H_f$ and $H_g$ proton signals were shifted in the $^{1}$H-NMR spectrum of BEECH. Here, $H_f$ shifted to 4.0 ppm from 3.33 ppm, and the methylene protons belonging to the piperazine ring resonated between 3.0 and 2.4 ppm along with the $H_g$ protons and the newly formed secondary hydroxyl hydrogens. Furthermore, the structure of BEECH was also confirmed with $^{13}$C-NMR (Fig. S3).

$^{1}$H-NMR and $^{13}$C-NMR of E-DOPO are presented in Figs. 2 and S4, respectively. Both spectra prove that E-DOPO was successfully synthesized. As can be seen from the $^{1}$H-NMR spectrum of E-DOPO, 8 protons of the DOPO moiety resonated between 8.0 and 7.0 ppm [54]. The characteristic allyl and aromatic protons of the eugenol were detected in the aforementioned chemical shifts.

The structure and purity of the synthesized monomers were further confirmed by mass and FTIR spectra. The m/z values for BEECH and E-DOPO were found to match the theoretical values and assure the purity of the synthesized monomers. The FTIR spectra of the synthesized monomers along with the 3SH and GBDA are presented in Fig. 3. The allyl bond stretching vibration bands of BEECH and E-DOPO were observed at around 1640 cm$^{-1}$. The bands at around 1600 cm$^{-1}$ were ascribed to the aromatic –C = C– vibrations. The vibration band seen in the FTIR spectrum of BEECH at 3319 cm$^{-1}$ was attributed to the hydroxyl stretching band of BEECH. Also, the absence of the bands associated with the oxirane ring of EECH at 840 and 760 cm$^{-1}$ in the spectrum of BEECH proves that the ring-opening reaction with piperazine took place.

Finally, the $^{31}$P-NMR spectrum of E-DOPO was recorded, which displayed a sharp single peak at 6.89 ppm (Fig. S5).

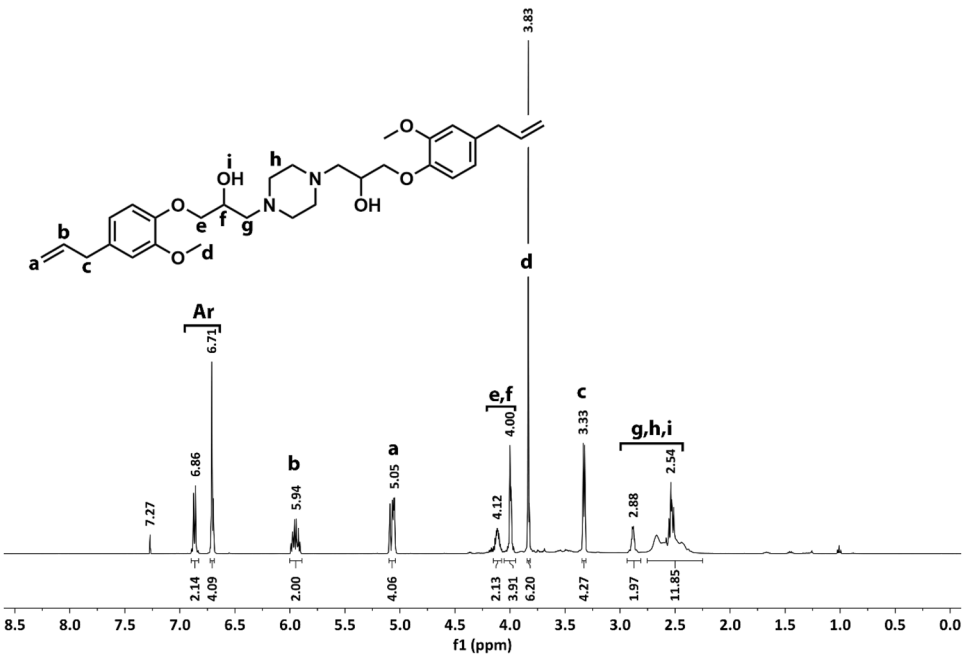


**Fig. 1** $^{1}$H-NMR spectrum of BEECH

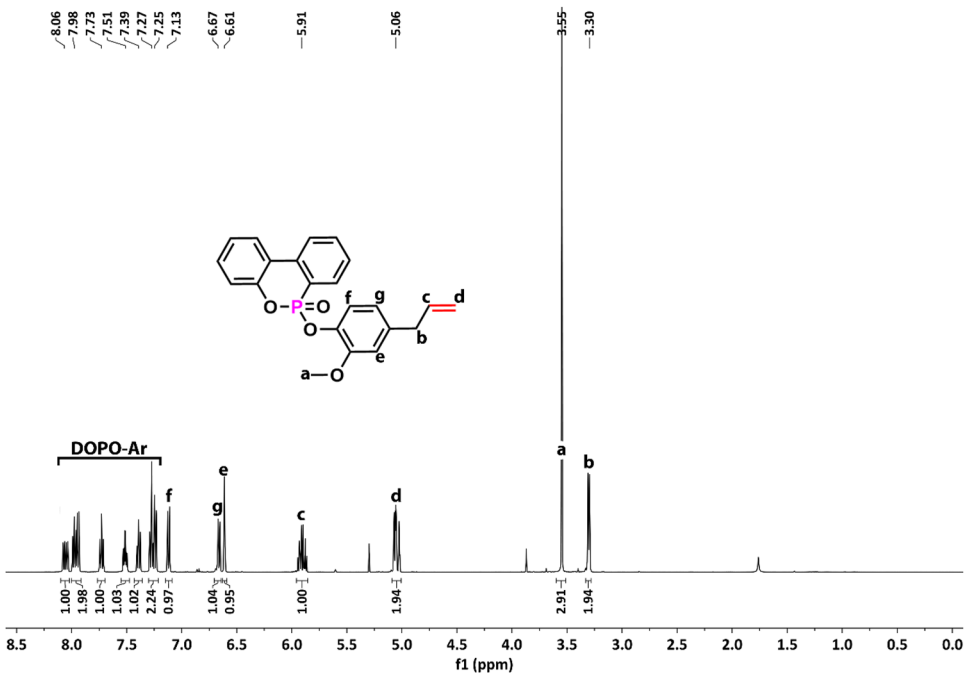


**Fig. 2** $^{1}$H-NMR spectrum of E-DOPO

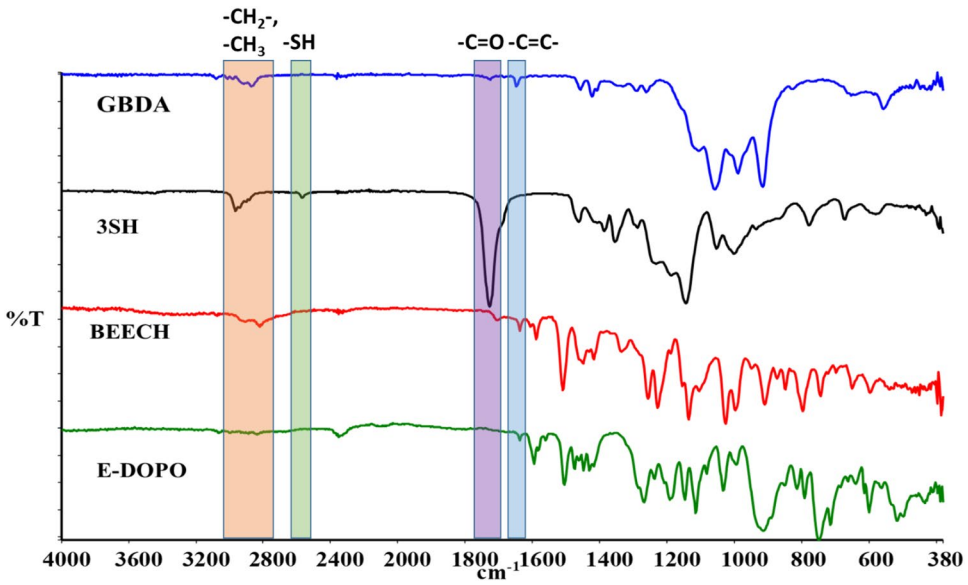


**Fig. 3** FTIR spectra of GBDA, 3SH, BEECH, and E-DOPO

## Characterization of the Photocured Thermosets

In this work, we prepared thermoset materials by using two commercial monomers; 3SH and GBDA, and two novel monomers; E-DOPO and BEECH. Our initial aim was to use BEECH as the main oligomer and eliminate the use of a petroleum-based allylic monomer (i.e. GBDA), however, the use of BEECH as the sole allylic oligomer led to partially cured, tacky films with poor mechanical properties when thick samples were prepared (> 300 µm). Only thin coatings could be prepared by using BEECH as the main oligomer. Therefore, we utilized GBDA as the main ene-monomer in this study. We chose GBDA as the main allyl component for the TEP system due to its low viscosity, high functionality, and its good compatibility with BEECH and E-DOPO monomers. Besides, we preferred GBDA over other commercial and widely used allyl monomers for TEP such as 1,3,5-triallyl-1,3,5-triazine-2,4,6(1H,3H,5H)-trione (TTT) to achieve a fully aliphatic base formulation that does not contain nitrogen atoms and rings. Thus, we aimed to test the performance of E-DOPO and BEECH on a highly flammable network with poor thermal stability.

The thermosets were structurally characterized by FTIR spectroscopy. Figure S6 displays the FTIR spectra

of the liquid precursor solutions before curing, and the photocured films, respectively. All formulations exhibited similar spectra. It can be seen from the spectra of the liquid precursors that both the thiol (2560 $cm^{-1}$) and allyl bands (1648 $cm^{-1}$) appear as very weak bands. When the aromatic E-DOPO and BEECH were added to the formulations, the characteristic bands at around 1600 $cm^{-1}$ were observed both in the FTIR spectra of the thermoset films and the precursor solutions. These vibration bands originate from the –C = C– bonds of the aromatic rings of E-DOPO and BEECH. Upon UV illumination, the thiol-ene reactions take place, and thiol groups react with the allyl functional groups via a photoinduced step-growth mechanism. As a result, both the thiol and allyl bands disappeared. This indicates that the photocuring process was conducted successfully [12, 14, 19].

We further evaluated the degree of curing by measuring the gel contents of the prepared thermosets. Gel content is a decisive criterion and an excellent indicator of the extent of curing. The gel content values of the compositions studied in this work are collected in Table 1. As can be seen, GT has a gel content value as high as 97%. When GBDA was partially replaced by E-DOPO, the gel contents started to decrease gradually. Similarly, the addition of BEECH also caused a decrease in the gel contents of the formulations. Thus it can be concluded that the UV light absorption of the aromatic units of E-DOPO and BEECH led to lower double bond conversions and in turn to lower gel content values [26, 27]. That's why we limited the percentages of E-DOPO and BEECH in the photocurable formulations. The UV spectra of the liquid mixtures were recorded and presented in Fig. S7. Another factor that limited the further use of E-DOPO is the crosslinking density. Since E-DOPO is a mono-functional monomer and TEP proceeds via radical-induced step-growth mechanism, we kept the level of E-DOPO below a threshold value to constitute a good level of crosslinking density.

In thiol-ene polymerization systems, the gel-point conversion (α) can be derived based on the functionality of the monomers according to the well-known Flory and Stockmayer equation [55–58]**:**

$$a = \sqrt{\frac{1}{r(f_{thiol}-1)(f_{ene}-1)}} \quad (1)$$

where, $f_{thiol}$ and $f_{ene}$ are the average functionalities and $r$ is the stoichiometric ratio.

According to this equation, the GT-encoded formulation containing a three-functional thiol and a four-functional allyl compound gels after 41% conversion. As the monofunctional E-DOPO and the two functional BEECH are introduced, the required theoretical gel-point conversion values increase as expected. The α values for GTE0.25, GTEB0.25, GTE0.5, GTE1.0, and GTEB1.0 were calculated to be 42.5, 43.6, 44.2, 47.7, and 52%, respectively.

These gel-point conversion results are in good accordance with the gel content values and clearly indicate that all the prepared formulations were converted to insoluble gels.

## Thermomechanical Properties

The thermomechanical properties of the thermosets were evaluated by DMA. The storage modulus ($E'$) and tanδ versus temperature plots are given in Fig. 4. The storage modulus values at 20 °C, crosslink densities ($\rho_x$), and tanδ values are reported in Table 2. The $\rho_x$ values of the networks were determined by using the following equation [10, 12].

$$\rho_x = \frac{E'}{2(1+\gamma)RT} \quad (2)$$

where $E'$ is the rubbery storage modulus at $Tg + 40$ °C in MPa, R is the gas constant (8.3145 J/mol K), T is the temperature in K and γ is Poisson's ratio. γ was assumed to be 0.5.

The storage modulus of GT was found as 26.5 MPa. It was previously reported that the $E'$ of thermoset materials

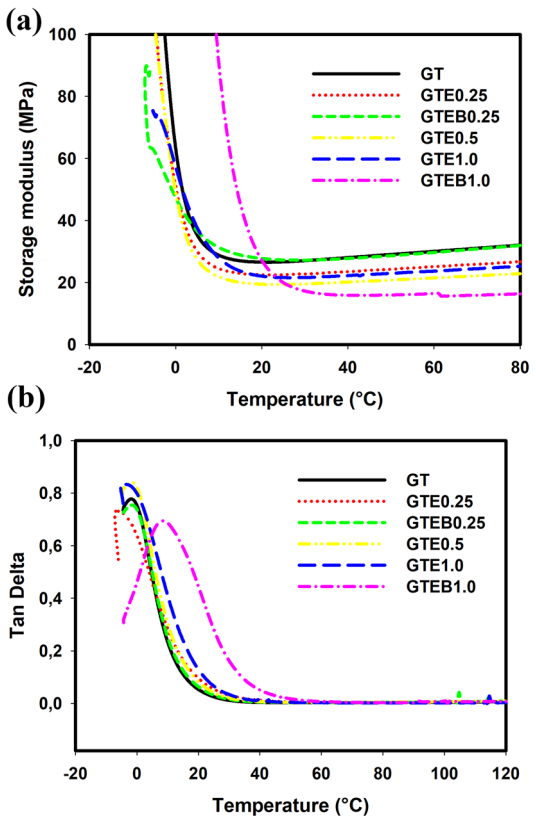


**Fig. 4** Storage modulus (**a**) and tanδ (**b**) curves of the photocured networks

**Table 2** Thermomechanical and thermal properties of the photocured resins

| | E′ (20 °C) MPa | $\rho_x$ (mol/m$^3$) | tanδ (°C) | $Tg^a$ (°C) | $T_1{}^b$ (°C) | $T_2{}^b$ (°C) | Char (%) | LOI (%) |
|---|---|---|---|---|---|---|---|---|
| GT | 26.5 | 3586 | − 1.5 | − 2.4 | 369 | 449 | 1.72 | 18.0 |
| GTE0.25 | 22.5 | 3011 | − 7.0 | − 5.9 | 362 | 455 | 2.10 | 18.8 |
| GTEB0.25 | 27.8 | 3572 | − 1.0 | 0.5 | 364 | 447 | 2.40 | 19.2 |
| GTE0.5 | 19.4 | 2581 | − 1.8 | − 5.5 | 369 | 445 | 4.65 | 19.8 |
| GTE1.0 | 22.0 | 2846 | − 3.8 | − 3.0 | 376 | 447 | 6.24 | 20.6 |
| GTEB1.0 | 27.5 | 1993 | 8.0 | 7.9 | 367 | 440 | 7.70 | 21.2 |

[a]Determined by DSC

[b]$T_1$ and $T_2$ are the maximum weight loss temperatures, which were determined from the maximum of the corresponding derivative curves

composed of GBDA and 4SH was 161 MPa [26]. This result indicates the effect of crosslinking on the stiffness of thiol-ene photocured thermosets. Previously, Liu et al., prepared hexa-allyl functional phosphazene monomer and prepared thiol-ene photocured novel thermosets by using 2, 3, or 4 functional thiols and found that the (E′) and tanδ values to depend on the functionality and rigidity of the monomers [59]. The partial replacement of GBDA with E-DOPO (GTE0.25) led to a decline in the storage modulus as a result of the decreased crosslinking density. Since E-DOPO is a monofunctional allyl monomer, the extent of crosslinking decreases. With the incorporation of di-allyl functional BEECH (GTEB0.25), both the crosslinking density and the storage modulus values increased. As expected, with further addition of E-DOPO (GTE0.5), the crosslinking density and the storage modulus values continued to decrease. However, when 1 mmol of E-DOPO was used (GTE1.0), the modulus slightly increased. This can be explained in terms of two antagonistic effects; the crosslinking density, and the rigidity/steric hindrance of the E-DOPO. As the amount of monofunctional allyl monomer; E-DOPO increases, the crosslinking density decreases and as a result the storage modulus values decrease. On the other hand, after a threshold value of E-DOPO within the formulations, its rigidity increases the stiffness of the thermosets, resulting in higher storage modulus values despite decreased crosslinking densities. The π–π stacking interactions of the E-DOPO increase as its concentration reaches to a relatively higher value and the extent of these interactions become the dominating factor that determines the modulus of the thermosets. In the case of GTEB1.0, the DMA results also showed a higher modulus value when compared to GT, despite an 80% decrease in the crosslinking density. Here, the rigid structures of E-DOPO and BEECH led to these increased modulus values, and also this situation can be attributed to the hydrogen bonding interactions stemming from BEECH.

The tanδ values which are often used instead of *Tgs* in literature followed almost a similar trend as the storage modulus of the thermosets. While the tanδ for GT was − 1.5 °C, a small amount of E-DOPO addition (GTE0.25), decreased the tanδ to − 7.0 °C. With the further addition of E-DOPO, tanδ was first increased (GTE0.5) and then slightly decreased (GTE1.0). The results revealed that the incorporation of difunctional BEECH increased the tanδ abruptly. This can be attributed to the hydrogen bonding attractions between the polymer chains when BEECH was used. It is known that hydrogen bonding results in a greater chain packing, increasing both *E′* and tanδ [60]. Even though the crosslinking density and the gel content values decreased with BEECH, the increased polarity of the networks led to strong intermolecular interactions which promoted the tanδ values.

## Thermal Properties of the Thermosets

The thermal stability of the thermosets was investigated using TGA and the *Tg*s of the networks were determined via DSC measurements. The TGA and the DSC results are listed in Table 2. The TGA curves of the thermosets are presented in Fig. 5. As can be seen from Fig. 5 all thermosets exhibit similar and two-step degradation profiles and negligible differences were detected for the first ($T_1$) and the second ($T_2$) maximum temperatures. $T_1$ and $T_2$ were found to be almost identical regardless of the composition of the thermosets. On the other hand, the char yields increased with increasing amounts of E-DOPO and BEECH. The results indicated a synergistic effect of the P- and N-containing monomers. 23% increase (from 6.24 to 7.7%) in the char yield was attained when BEECH was introduced to GTE1.0. When compared to GT, GTEB1.0 displayed approximately 4.5 times higher char yield. These results certainly show the effectiveness of E-DOPO and BEECH for the enhancement of thermal properties.

The DSC spectra of the thermosets are given in Fig. S8. The measured *Tg* values are in good accordance with the DMA results. Often the measured values of tanδ and *Tg* of polymers vary since the instruments, and the methods are different. Therefore, the slight differences between the *Tg* values obtained by DSC and the tanδ values obtained by DMA are reasonable. The *Tg* of GT was found as − 2.4 °C.

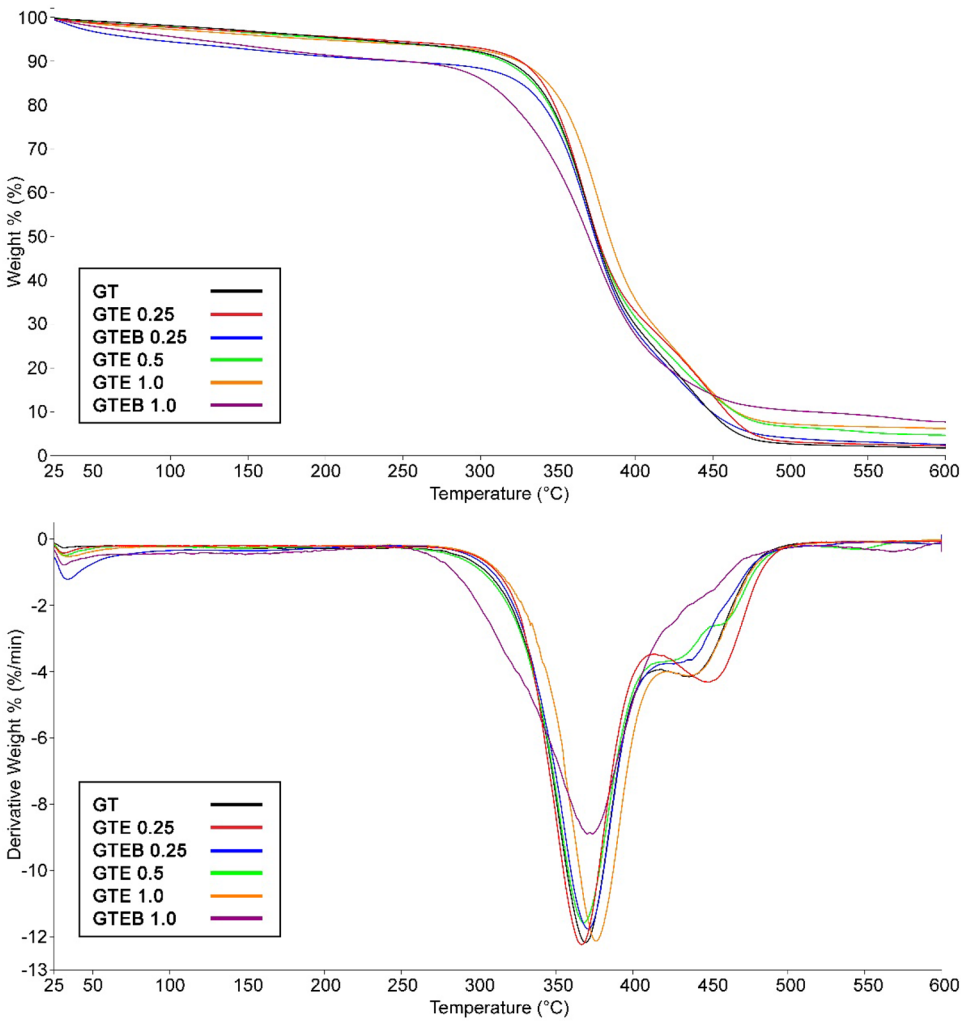


**Fig. 5** TGA thermograms (**a**) and the derivative weight curves of the photocured thermosets (**b**)

The monofunctional E-DOPO first decreased the *Tg* to − 5.9 °C (GTE0.25) and then the *Tg* values slightly increased with increasing amounts of E-DOPO, reaching − 5.5 °C and − 3.0 °C for GTE0.5 and GTE1.0, respectively. Similar to DMA results, the addition of BEECH significantly improved the *Tg* values and the *Tg* of GTEB0.25 was found as 0.5 °C. The highest amount of BEECH-containing thermoset displayed the highest *Tg* among other formulations and the *Tg* of GTEB1.0 was found as 7.9. It was previously reported that multifunctional eugenol-based monomers display high *Tg* values [47]. The increase in the *Tg* with the increasing amount of BEECH can be attributed to its hydrogen bonding ability, which increases the interactions between polymer chains, forms physical crosslinks and reduces the free volume.

The LOI values were investigated and the results are listed in Table 2. The base formulation; GT was found to be highly flammable (LOI:18.0%). This low fire resistance was attributed to the aliphatic nature of the monomers; 3SH and GBDA. The flexible thioether bonds which are highly susceptible to degradation in these thermosets also accelerate the burning process. When only 3.9% E-DOPO was introduced, the LOI value increases to 18.8%.

The addition of BEECH to this formulation (GTEB0.25) led to a slight increase in the LOI value and it reached 19.2%. When the E-DOPO as well as the phosphorous percentage was doubled in the formulations (GTE0.5), the 10% increase was obtained for the LOI values with respect to the base formulation. The increase in the P percentage to 1.18%, led to an LOI value of 20.6% which further increased to 21.2% with the incorporation of BEECH. The total enhancement in the LOI value was found as ~ 17.8%.

The obtained LOI values were found to be low in this work when compared to the literature. While the main reason for these lower values can be attributed to the highly flammable characteristics of the base formulation, the results demonstrated that E-DOPO is effective in improving the flame retardancy. With only 12.3% of E-DOPO (corresponding to 1% P), the improvement in the LOI values was over 14%. This degree of improvement

is good considering the amount of N and P within the polymer matrix. There is no doubt that the LOI values would be higher if a relatively higher fire–resistant base polymer matrix was used. For instance, Zhang et al., prepared a similar monomer to E-DOPO in two steps [53]. First, they synthesized EECH and then reacted it with DOPO to give a new bio-based flame retardant, DOPO-GE. DOPO-GE was blended with a commercial bisphenol A epoxy resin and 4,4′-diamino diphenyl sulfone as the curing agent. The LOI value of the 1.0% P- and 2.46% N-containing thermosets was measured as 32.5%. In contrast to the LOI value of the DOPO-GE-free pristine resin, the LOI value was 22.6%. Here, both the fire resistance of the highly aromatic base formulation and the relatively higher degree of P and N percentages in the formulations contributed to these high LOI values.

The literature on flame retardant P-containing monomers showed that these compounds act both in the gas and condensed phases [27, 38, 61, 62]. Upon decomposition of these monomers, P-containing radical species which entrap the free radicals are released into the gas phase and thereby reducing the progress of the flames. Furthermore, N-containing gases are also released (if the monomer constitutes any) and they act in such a way to decrease the oxygen concentration in the gas phase. In the condensed phase, the decomposition of the phosphorous monomers leads to the generation of P-containing acidic substances which catalyze the carbonization and char formation. The formation of a dense char layer impedes the transfer of heat and oxygen and as a result, the unburnt portion of the polymer matrix is protected and becomes fire-proof.

## Wettability of the Photocured Networks

The hydrophilic/hydrophobic character of the thermoset films was assessed by measuring the contact angle values. The average contact angle values of the photocured thermosets are presented in Fig. 6 along with the images which best represent the given CA value. When approximately 8 molar percent of GBDA was replaced by E-DOPO, the CA was decreased to 65° from 68°. This was attributed to the polarity of the phosphorous groups. As expected, the polar –OH groups and tertiary amine groups of BEECH, also led to a decline in the CA values.

The CA value of GTEB0.25 was found as 62°. With further addition of either E-DOPO and/or BEECH, the CA values slightly decreased. It must be noted here that the change in the CA values of the thermosets was not very significant. Thus, it can be said that all the prepared thermosets have hydrophilic surfaces.

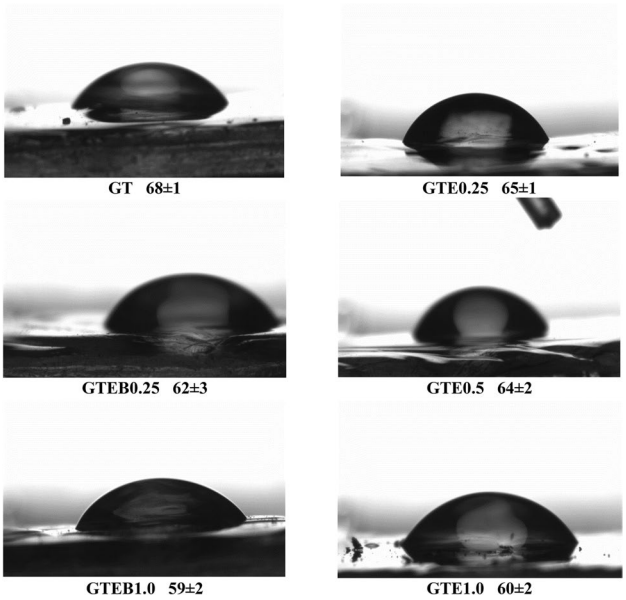


**Fig. 6** WCA values of the photocured films

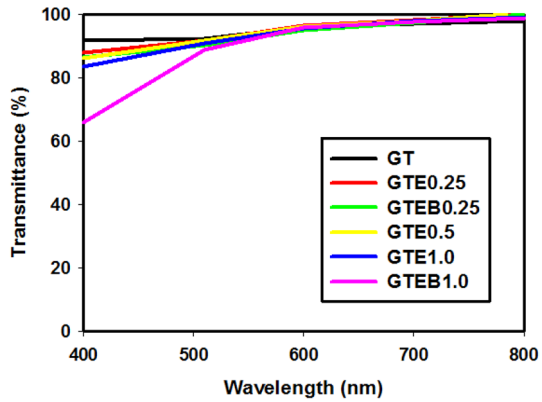


**Fig. 7** Transmission spectra of the thiol-ene photocured networks (not all points are shown for clarity)

## Optical Properties

The light transmission percentage of photocurable materials determines whether these materials are suitable for optical applications and transparent coatings. The BEECH- and E-DOPO-containing free-films were yellow as opposed to GT which is composed of only fully aliphatic 3SH and GBDA monomers. The transmittance spectra of the prepared materials are given in Fig. 7. All films exhibited similar behaviors in terms of light transmittance and high light transmission in the region between 800 and 400 nm. Only a slight decrease was observed as the amount of BEECH and E-DOPO were increased in the formulations except for the GTE1.0 formulation, which displayed relatively lower

light transmittance percentage values, especially within 500–400 nm range. This decrease in light transmission can be attributed to the absorption of light by these monomers bearing aromatic units.

## Conclusion

Here, we synthesized a novel bio-based allyl-functionalized P-containing monomer. The monomer was prepared in a one-pot, one-step reaction. Furthermore, another bio-based diallyl compound containing nitrogen was prepared. The synthesized monomers were used to prepare thiol-ene photocurable networks. The main conclusions of this work are as follows:

(1) Two novel eugenol-based monomers were synthesized and characterized.
(2) All prepared thermosets displayed gel contents over 88%.
(3) The addition of the newly synthesized monomers especially, the diallyl compound (BEECH) improved the storage modulus values as well as the glass transition temperatures.
(4) The char yields increased with an increasing amount of E-DOPO.
(5) The LOI value of the base formulation was improved by the synergism of the P- and N-containing monomers and up to 17.8% improvement was achieved. The LOI of the base formulation was raised to 21.2% from 18.0% with the aid of the newly synthesized monomers.
(6) The E-DOPO and BEECH addition increased the hydrophilicity of the thermosets.
(7) All films exhibited high light transmittance over ~ 90% in the region between 800 and 500 nm.

The renewable and inherent non-toxic properties of bio-based green monomers render them potential alternatives to replace commercial monomers. We anticipate that in the future, E-DOPO or its derivatives will be used in several applications.

**Supplementary Information** The online version contains supplementary material available at https://doi.org/10.1007/s10924-023-02813-1.

**Author Contributions** OO: Investigation, EÇ: Investigation, Conceptualization, Writing—Original Draft, GS: Investigation, USG: Reviewing and Editing, HD: Conceptualization, Methodology, Reviewing and Editing, VK: Investigation, Conceptualization, Writing—Original Draft.

**Funding** This work was supported by the Scientific Research Projects Department of Istanbul Technical University (ITU-BAP) (Project number: TGA-2022-43637).

## Declarations

**Conflict of interest** The authors declare no conflicts of interest.

## References

1. Gandini A, Lacerda TM, Carvalho AJ, Trovatti E (2016) Progress of polymers from renewable resources: furans, vegetable oils, and polysaccharides. Chem Rev 116(3):1637–1669
2. Iwata T (2015) Biodegradable and bio-based polymers: future prospects of eco-friendly plastics. Angew Chem Int Ed 54(11):3210–3215
3. Kristufek SL, Wacker KT, Tsao YYT, Su L, Wooley KL (2017) Monomer design strategies to create natural product-based polymer materials. Nat Prod Rep 34(4):433–459
4. Ghasemlou M, Daver F, Ivanova EP, Adhikari B (2019) Bio-based routes to synthesize cyclic carbonates and polyamines precursors of non-isocyanate polyurethanes: a review. Eur Polym J 118:668–684
5. Zhang C, Garrison TF, Madbouly SA, Kessler MR (2017) Recent advances in vegetable oil-based polymers and their composites. Prog Polym Sci 71:91–143
6. Medway AM, Sperry J (2014) Heterocycle construction using the biomass-derived building block itaconic acid. Green Chem 16(4):2084–2101
7. Gandini A, Lacerda TM (2015) From monomers to polymers from renewable resources: recent advances. Prog Polym Sci 48:1–39
8. Kumar B, Agumba DO, Pham DH, Kim HC, Kim J (2022) Recent progress in bio-based eugenol resins: from synthetic strategies to structural properties and coating applications. J Appl Polym Sci 139(2):51532
9. Çakmakçı E, Özdemir M, Şen F, Bulut M, Yalçın B (2022) Vegetable oil-based, coumarin-containing antibacterial thermosets with improved thermal stability via copper-free thermal azide-alkyne click polymerization. Ind Crops Prod 182:114870
10. Cangul K, Cakmakci E, Daglar O, Gunay US, Hizal G, Tunca U, Durmaz H (2022) Metal-free click modification of triple bond-containing polyester with azide-functionalized vegetable oil: plasticization and tunable solvent adsorption. ACS Omega 58:1105
11. Şeker H, Çakmakçi E (2020) Fully bio-based thiol-ene photocured thermosets from isosorbide and tung oil. J Polym Sci 58(8):1105–1114
12. Cakmakci E, Sen F, Kahraman MV (2019) Isosorbide diallyl based antibacterial thiol–ene photocured coatings containing polymerizable fluorous quaternary phosphonium salt. ACS Sustain. Chem. Eng 7(12):10605–10615
13. Aricò F (2020) Isosorbide as biobased platform chemical: recent advances. Curr Opin Green Sustain Chem 21:82–88
14. Oktay B, Çakmakçi E (2017) DOPO tethered Diels Alder clickable reactive silica nanoparticles for bismaleimide containing flame retardant thiol-ene nanocomposite coatings. Polymer 131:132–142
15. Niu HX, Ding HL, Huang JL, Wang X, Song L, Hu Y (2022) A furan-based phosphaphenanthrene-containing derivative as a highly efficient flame-retardant agent for epoxy thermosets without deteriorating thermomechanical performances. Chin J Polym Sci 40(3):233–240
16. Ma J, Li G, Hua X, Liu N, Liu Z, Zhang F, Ao Y (2022) Biodegradable epoxy resin from vanillin with excellent flame-retardant and outstanding mechanical properties. Polym Degrad Stab 201:109989
17. Ma T, Li L, Mei C, Wang Q, Guo C (2022) Synthesis of a vanillin-based curing agent and its application in wood to improve dimensional stability and flame retardancy. Polym Adv Technol 33:3249

18. Yin GZ, Yang XM, Hobson J, López AM, Wang DY (2022) Bio-based poly (glycerol-itaconic acid)/PEG/APP as form stable and flame-retardant phase change materials. Compos Commun 30:101057
19. Çakmak Y, Çakmakçi E, Apohan NK, Karadag R (2022) Isosorbide, pyrogallol, and limonene-containing thiol-ene photocured bio-based organogels for the cleaning of artworks. J Cult Herit 55:391–398
20. Harvey BG, Guenthner AJ, Yandek GR, Cambrea LR, Meylemans HA, Baldwin LC, Reams JT (2014) Synthesis and characterization of a renewable cyanate ester/polycarbonate network derived from eugenol. Polymer 55(20):5073–5079
21. Qin J, Liu H, Zhang P, Wolcott M, Zhang J (2014) Use of eugenol and rosin as feedstocks for biobased epoxy resins and study of curing and performance properties. Polym Int 63(4):760–765
22. Hu Y, Tian Y, Cheng J, Zhang J (2020) Synthesis of eugenol-based polyols via thiol–ene click reaction and high-performance thermosetting polyurethane therefrom. ACS Sustain Chem Eng 8(10):4158–4166
23. Tian Y, Wang Q, Cheng J, Zhang J (2020) A fully biomass based monomer from itaconic acid and eugenol to build degradable thermosets via thiol–ene click chemistry. Green Chem 22(3):921–932
24. Hoyle CE, Bowman CN (2010) Thiol–ene click chemistry. Angew Chem Int Ed 49(9):1540–1573
25. Lowe AB (2010) Thiol-ene "click" reactions and recent applications in polymer and materials synthesis. Polym Chem 1(1):17–36
26. Daglar O, Çakmakçi E, Gunay US, Hizal G, Tunca U, Durmaz H (2021) Acetylene dicarboxylic acid diallyl ester: a versatile monomer for thiol-ene photocured networks. Macromol Mater Eng 306:2100427
27. Sagdic G, Cakmakci E, Daglar O, Gunay US, Hizal G, Tunca U, Durmaz H (2022) Thermal and mechanical properties of thiol-ene photocured thermosets containing DOPO-based liquid reactive flame retardant synthesized by metal-free azide-alkyne click reaction. Prog Org Coat 167:106825
28. Kazybayeva DS, Irmukhametova GS, Khutoryanskiy VV (2021) Thiol-ene "click reactions" as a promising approach to polymer materials. Polym. Sci. Series B 2021:1–16
29. Guo W, Liang F, Chen S, Yu K, Sun J, Pang Z, Fei B (2022) Magnolol-derived thiol-ene photo-polymerized membranes with intrinsic anti-flammability and high transparency. Compos B Eng 242:110074
30. Machado TO, Sayer C, Araujo PH (2017) Thiol-ene polymerisation: a promising technique to obtain novel biomaterials. Eur Polym J 86:200–215
31. Cheng C, Zhang X, Chen X, Li J, Huang Q, Hu Z, Tu Y (2016) Self-healing polymers based on eugenol via combination of thiol-ene and thiol oxidation reactions. J Polym Res 23(6):1–12
32. Shibata M, Tetramoto N, Imada A, Neda M, Sugimoto S (2013) Bio-based thermosetting bismaleimide resins using eugenol, bieugenol and eugenol novolac. React Funct Polym 73(8):1086–1095
33. Hu K, Zhao D, Wu G, Ma J (2015) Polyesters derived from bio-based eugenol and 10-undecenoic acid: synthesis, characterization, and structure–property relationships. RSC Adv 5(105):85996–86005
34. Dai J, Jiang Y, Liu X, Wang J, Zhu J (2016) Synthesis of eugenol-based multifunctional monomers via a thiol–ene reaction and preparation of UV curable resins together with soybean oil derivatives. RSC Adv 6(22):17857–17866
35. Guzman D, Ramis X, Fernandez-Francos X, De la Flor S, Serra A (2017) New bio-based materials obtained by thiol-ene/thiol-epoxy dual curing click procedures from eugenol derivates. Eur Polym J 93:530–544
36. Modjinou T, Versace DL, Abbad-Andallousi S, Bousserrhine N, Dubot P, Langlois V, Renard E (2016) Antibacterial and antioxidant bio-based networks derived from eugenol using photo-activated thiol-ene reaction. React Funct Polym 101:47–53
37. Dai J, Ma S, Zhu L, Wang S, Yang L, Song Z, Zhu J (2017) UV-thermal dual cured anti-bacterial thiol-ene networks with superior performance from renewable resources. Polymer 108:215–222
38. Cakmakci E, Kahraman MV (2015) Boron/Phosphorus-containing flame-retardant photocurable coatings. Photocured Mater 108:150–187
39. Sonnier R, Taguet A, Ferry L, Lopez-Cuesta JM (2018) Towards bio-based flame retardant polymers. Springer International Publishing, pp 33–72
40. Hobbs CE (2019) Recent advances in bio-based flame retardant additives for synthetic polymeric materials. Polymers 11(2):224
41. Costes L, Laoutid F, Brohez S, Dubois P (2017) Bio-based flame retardants: when nature meets fire protection. Mater Sci Eng R Rep 117:1–25
42. Morgan AB, Cusack PA, Wilkie CA (2021) Other non-halogenated flame retardants and future fire protection concepts & needs. Non-halogenated flame retardant handbook. Wiley, pp 475–554
43. Ecochard Y, Decostanzi M, Negrell C, Sonnier R, Caillol S (2019) Cardanol and eugenol based flame retardant epoxy monomers for thermostable networks. Molecules 24(9):1818
44. Decostanzi M, Tavernier R, Fontaine G, Bourbigot S, Negrell C, Caillol S (2019) Eugenol-based thermally stable thermosets by Alder-ene reaction: from synthesis to thermal degradation. Eur Polym J 117:337–346
45. Liu J, He Z, Wu G, Zhang X, Zhao C, Lei C (2020) Synthesis of a novel nonflammable eugenol-based phosphazene epoxy resin with unique burned intumescent char. Chem Eng J 390:124620
46. Li C, Wan J, Kalali EN, Fan H, Wang DY (2015) Synthesis and characterization of functional eugenol derivative based layered double hydroxide and its use as a nanoflame-retardant in epoxy resin. J. Mater. Chem. A 3(7):3471–3479
47. Faye I, Decostanzi M, Ecochard Y, Caillol S (2017) Eugenol bio-based epoxy thermosets: from cloves to applied materials. Green Chem 19(21):5236–5242
48. Miao JT, Ge M, Wu Y, Chou TY, Wang H, Zheng L, Wu L (2020) Eugenol-derived reconfigurable high-performance epoxy resin for self-deployable smart 3D structures. Eur Polym J 134:109805
49. Pourchet S, Sonnier R, Ben-Abdelkader M, Gaillard Y, Ruiz Q, Placet V, Boni G (2019) New reactive isoeugenol based phosphate flame retardant: toward green epoxy resins. ACS Sustain. Chem Eng 7(16):14074–14088
50. Miao JT, Yuan L, Guan Q, Liang G, Gu A (2018) Water-phase synthesis of a biobased allyl compound for building uv-curable flexible thiol–ene polymer networks with high mechanical strength and transparency. ACS Sustain Chem Eng 6(6):7902–7909
51. Miao JT, Yuan L, Liang G, Gu A (2019) Biobased bismaleimide resins with high renewable carbon content, heat resistance and flame retardancy via a multi-functional phosphate from clove oil. Mater Chem Front 3(1):78–85
52. Liu B, Chen J, Liu N, Ding H, Wu X, Dai B, Kim I (2020) Bio-based polyesters synthesized by ring-opening copolymerizations of eugenyl glycidyl ether and cyclic anhydrides using a binuclear [OSSO] CrCl complex. Green Chem 22(17):5742–5750
53. Zhang D, Yang C, Ran H, Wang J, Wan J, Li Y, Hu D (2022) A new DOPO-eugenol adduct as an effective flame retardant for epoxy thermosets with improved mechanical properties. J Renew Mater 10(7):1797
54. Ma S, Liu X, Jiang Y, Fan L, Feng J, Zhu J (2014) Synthesis and properties of phosphorus-containing bio-based epoxy resin from itaconic acid. Sci China Chem 57(3):379–388
55. Higham AK, Garber LA, Latshaw DC, Hall CK, Pojman JA, Khan SA (2014) Gelation and cross-linking in multifunctional thiol and multifunctional acrylate systems involving an in situ comonomer catalyst. Macromolecules 47(2):821–829

56. Fairbanks BD, Scott TF, Kloxin CJ, Anseth KS, Bowman CN (2009) Thiol− yne photopolymerizations: Novel mechanism, kinetics, and step-growth formation of highly cross-linked networks. Macromolecules 42(1):211–217
57. Flory PJ (1941) Molecular size distribution in three dimensional polymers I. Gelation. J Am Chem Soc 63(11):3083–3090
58. Stockmayer WH (1943) Theory of molecular size distribution and gel formation in branched-chain polymers. J Chem Phys 11(2):45–55
59. Liu T, Sun L, Ou R, Fan Q, Li L, Guo C, Wang Q (2019) Flame retardant eugenol-based thiol-ene polymer networks with high mechanical strength and transparency. Chem Eng J 368:359–368
60. Miao JT, Yuan L, Guan Q, Liang G, Gu A (2017) Biobased heat resistant epoxy resin with extremely high biomass content from 2, 5-furandicarboxylic acid and eugenol. ACS Sustain Chem Eng 5(8):7003–7011
61. Schartel B (2010) Phosphorus-based flame retardancy mechanisms—old hat or a starting point for future development? Materials 3(10):4710–4745
62. Markwart JC, Battig A, Zimmermann L, Wagner M, Fischer J, Schartel B, Wurm FR (2019) Systematically controlled decomposition mechanism in phosphorus flame retardants by precise molecular architecture: P–O vs P–N. ACS Appl Polym Mater 1(5):1118–1128